

ACCEPTED MANUSCRIPT

Conductance quantisation in patterned gate $\text{In}_{0.75}\text{Ga}_{0.25}\text{As}$ structures up to $6 \times (2e^2/h)$

To cite this article before publication: Yilmaz Gul *et al* 2019 *J. Phys.: Condens. Matter* in press <https://doi.org/10.1088/1361-648X/aafd05>

Manuscript version: Accepted Manuscript

Accepted Manuscript is “the version of the article accepted for publication including all changes made as a result of the peer review process, and which may also include the addition to the article by IOP Publishing of a header, an article ID, a cover sheet and/or an ‘Accepted Manuscript’ watermark, but excluding any other editing, typesetting or other changes made by IOP Publishing and/or its licensors”

This Accepted Manuscript is © 2019 IOP Publishing Ltd.

During the embargo period (the 12 month period from the publication of the Version of Record of this article), the Accepted Manuscript is fully protected by copyright and cannot be reused or reposted elsewhere.

As the Version of Record of this article is going to be / has been published on a subscription basis, this Accepted Manuscript is available for reuse under a CC BY-NC-ND 3.0 licence after the 12 month embargo period.

After the embargo period, everyone is permitted to use copy and redistribute this article for non-commercial purposes only, provided that they adhere to all the terms of the licence <https://creativecommons.org/licenses/by-nc-nd/3.0>

Although reasonable endeavours have been taken to obtain all necessary permissions from third parties to include their copyrighted content within this article, their full citation and copyright line may not be present in this Accepted Manuscript version. Before using any content from this article, please refer to the Version of Record on IOPscience once published for full citation and copyright details, as permissions will likely be required. All third party content is fully copyright protected, unless specifically stated otherwise in the figure caption in the Version of Record.

View the [article online](#) for updates and enhancements.

Conductance Quantisation in patterned gate $\text{In}_{0.75}\text{Ga}_{0.25}\text{As}$ structures up to $6 \times (2e^2/h)$

Y Gul^{1(*)}, G L Creeth¹, D English¹, S N Holmes², K J Thomas^{1(†)}, I Farrer³,

D J Ellis², D A Ritchie⁴ and M Pepper¹

¹London Centre for Nanotechnology, University College London,
17-19 Gordon Street, London WC1H 0AH, UK

²Toshiba Research Europe Ltd, Cambridge Research Laboratory,
208 Cambridge Science Park, Milton Road, Cambridge CB4 0GZ, UK

³Department of Electronic and Electrical Engineering, University of Sheffield,
Mappin Street, Sheffield S1 3JD, UK

⁴Cavendish Laboratory, University of Cambridge, J J Thomson Avenue,
Cambridge CB3 0HE, UK

Abstract

We present electrical measurements from $\text{In}_{0.75}\text{Ga}_{0.25}\text{As}$ 1-dimensional channel devices with Rashba-type, spin-orbit coupling present in the 2-dimensional contact regions. Suppressed backscattering as a result of the time-reversal asymmetry at the 1-dimensional channel entrance results in enhanced ballistic transport characteristics with clear quantised conductance plateaus up to $6 \times (2e^2/h)$. Applying D.C. voltages between the source and drain ohmic contacts and an in-plane magnetic field confirms a ballistic transport picture. For asymmetric patterned gate biasing, a lateral spin-orbit coupling effect is weak. However, the Rashba-type spin-orbit coupling leads to a g-factor in the 1-dimensional channel that is reduced in magnitude from the 2-dimensional value of 9 to ~ 6.5 in the lowest subband when the effective Rashba field and the applied magnetic field are perpendicular.

*Email: y.gul@ucl.ac.uk

1
2
3
4
5 ORCID id

6
7 S. N. Holmes: <https://orcid.org/0000-0003-2776-357x>

8
9 M. Pepper: <https://orcid.org/0000-0003-3052-5425>

10
11
12
13
14
15 (†) Present address, Department of Physics, Central University of Kerala, Riverside
16 Transit Campus, Padannakkad, Kerala, 671314 India
17
18
19
20
21
22
23
24
25
26
27
28
29
30
31
32
33
34
35
36
37
38
39
40
41
42
43
44
45
46
47
48
49
50
51
52
53
54
55
56
57
58
59
60

1. Introduction

The limitations of conventional electronic devices can be overcome by implementing spin-based electronics where the spin degree of freedom plays the central role [1]. Ballistic transport in semiconductor nanowires is essential for applications in quantum logic devices [2] and utilising electron spin to encode logical information also paves the way for quantum computing [3]. However, many challenges must be overcome, such as injection, manipulation and detection of spin-polarised currents. For this to be achieved, materials with high spin-orbit coupling are being investigated as this is a possible mechanism for spin control without ferromagnetic contacts or large applied magnetic fields. Rashba-type spin-orbit coupling [4-6] could achieve electrical spin control and generation of spin-polarised current without the use of ferromagnetic contacts [7]. The Rashba spin-orbit coupling effect arises when an electron moves (with in plane wave vector components k_x, k_y) in an asymmetric potential at a heterojunction interface with

Rashba coefficient (α). An effective magnetic field exists, $\mathbf{B}_R = \frac{2\alpha(k_y, -k_x, 0)}{g^* \mu_B}$ where

μ_B is the Bohr Magneton and g^* is the effective g-factor. This effective field lies in the plane of the 2-dimensional electron gas (2DEG) and is perpendicular to \mathbf{k} . The precession of the electron spin can be modulated by adjusting the gate voltage to tune the confinement potential and hence α associated with the heterojunction. $\text{In}_x\text{Ga}_{1-x}\text{As}$ -based materials are ideal to study spin effects as the band structure is dominated by Rashba spin-orbit coupling induced by structural inversion asymmetry (SIA) at zero magnetic field [8]. The low electron effective mass (m^*) of $0.040 m_e$ (m_e is the free electron mass, see reference [9]) in $\text{In}_{0.75}\text{Ga}_{0.25}\text{As}$ also results in high electron mobilities and large 1-dimensional subband energy spacing. These characteristics make this material system a promising candidate for ballistic spintronics devices in 1-dimension.

Patterned gate devices that define a quantum wire in the 2DEG system are an effective way to study 1-dimensional transport, from a picture of non-interacting states [10, 11] to many body effects driven by electron-electron interaction [12]. Conductance quantisation has been demonstrated in high mobility GaAs devices, yet the small effective g-factor ($|g^*|=0.44$) and weak spin-orbit coupling make it difficult to observe spin-polarisation

phenomena without the application of an external magnetic field. The g -factor for $\text{In}_x\text{Ga}_{1-x}\text{As}$ devices with $x > 0.5$ is $|g^*| \sim 8$ and for the case of $\text{In}_{0.75}\text{Ga}_{0.25}\text{As}$ $|g^*| = 9.1 \pm 0.1$ [13]. A summary of the initial spin transport measurements on undoped $\text{In}_{0.75}\text{Ga}_{0.25}\text{As}$ quantum wells and 1-dimensional channels were published in reference [14].

The outline of this article is as follows. The methods of fabricating and measuring the devices are described in Section 2. We then introduce the device characterisation and properties of 1-dimensional conductance in Section 3. We measure the device conductance when a D.C. voltage is applied to the source and the drain ohmic contacts and outline the method of obtaining an effective g factor in Section 3 C. In Section 4 the experimental data is summarised.

2. Methods

Standard Hall bars were processed from modulation doped, high electron mobility transistor (HEMT) structures. Au-Ge-Ni ohmic contacts were deposited using thermal evaporation and annealed at 450 °C for 120 s. The patterned gates were fabricated using electron beam lithography with Ti/Au metallisation. The device had a mobility of 2.9×10^5 $\text{cm}^2/\text{V}\cdot\text{s}$ (at a carrier density of 2.3×10^{11} cm^{-2}) in the dark and 4.3×10^5 $\text{cm}^2/\text{V}\cdot\text{s}$ (at 3.7×10^{11} cm^{-2}) after brief in-situ illumination at 4.2 K. Studies on modelling [15] the mobilities in the $\text{In}_{0.75}\text{Ga}_{0.25}\text{As}$ wafers used in this work have taken into account four different scattering mechanisms, background impurities, remote (modulated doped) impurity, alloy disorder and interface roughness scattering. It was found that alloy disorder becomes more important as the carrier density increases before the on-set of intersubband scattering at carrier density of $> 3.7 \times 10^{11}$ cm^{-2} . The patterned gates have a length (L) of 200 nm and a width (W) of 400 nm. The gates are insulated from the $\text{In}_{0.75}\text{Al}_{0.25}\text{As}$ barrier with 50 nm of SiO_2 dielectric. This is required as there is no Schottky barrier between metal gates deposited on the surface and the 2DEG [16]. The patterned gate devices were measured in a dilution fridge with a base temperature of 50 mK. Figure 1 shows the conductance on cooling from 4.2 K to 50 mK as the patterned gate voltage is swept to 0 V from depletion. An A.C. voltage of 100 μV was applied between the source and the drain during cool down. The device was briefly illuminated at

1
2
3 4.2 K in order to get a conductance (G) of $1000 \mu\text{S}$. This corresponds to an electron
4 density of $3.7 \times 10^{11} \text{ cm}^{-2}$.
5
6

7 **3. Experimental results and discussion**

8 **A. Device initialisation**

9
10
11
12
13 In order to observe ballistic conductance quantisation the width of the channel must be
14 comparable to the Fermi wavelength and the temperature must be low compared to the
15 characteristic energy spacing of the 1-dimensional subbands in the channel. The electron
16 mean free path (λ) which is $2.3 \mu\text{m}$ at $2.3 \times 10^{11} \text{ cm}^{-2}$ must be $\gg L$, the channel length.
17 Background impurities can lead to scattering in the channel and quasi-ballistic transport.
18 In previous work [17] telegraph noise was identified as causing the conductance to vary
19 by steps of $\sim e^2/h$ in etched InAs quantum point contacts with a low mobility of 65×10^3
20 $\text{cm}^2/\text{V.s}$. The background impurity density in the wafer studied here is $\sim 5.6 \times 10^{15} \text{ cm}^{-3}$
21 [15] which results in an average impurity spacing of $\sim 60 \text{ nm}$ and narrow patterned gate
22 separations are needed to avoid the effects of quasi-ballistic transport. The effective
23 potential profile of the 1-dimensional channel was shown to vary based on a study of 256
24 lithographically identical split-gates [18].
25
26
27
28
29
30
31
32
33

34
35 The strong spin-orbit coupling in these systems suppresses backscattering due to the
36 weak anti-localisation effect [19] leading to enhanced conductivity and clear ballistic
37 transport. This is demonstrated experimentally here where we observe quantised
38 conductance up to $6 \times G_0$ ($G_0 = 2e^2/h$) see figure 1. A series resistance corresponding to
39 the channel resistance at patterned gate voltage ($V_{\text{sg}} = 0 \text{ V}$), is removed to calculate the
40 ballistic conductance of the channel. The conductance in figure 1 also shows a $0.7 \times G_0$
41 structure which is widely accepted to be spin related [20, 21]. The $0.7 \times G_0$ structure is
42 more pronounced at 4.2 K [20] although the origin of the $0.7 \times G_0$ anomaly is still unclear
43 with explanations varying from ferromagnetic spin-coupling [22], to Wigner
44 crystallisation [12] to the influence of inelastic scattering [23, 24].
45
46
47
48
49
50
51
52

53 **B. Finite source drain voltage**

54
55
56 Measurements were made at 50 mK with a D.C. source drain bias. This caused additional
57
58
59
60

plateaus to appear at half integer values $(N \pm 1/2) \times G_0$ [25, 26] where N is an integer. However, the half integer plateaus reported here are significantly clearer than in the earlier studies and requires no external magnetic field [26, 27]. To fully investigate this phenomenon D.C. bias spectroscopy was performed on the device, stepping the D.C. bias (V_{sd}) from 8 mV to -8 mV in 0.025 mV increments. This can be seen in figure 2. A clear feature of this D.C. bias spectroscopy is the fact that it is asymmetric between positive and negative bias. While positive D.C. source drain bias has a $0.5 \times G_0$ structure that stays strong with increasing D.C. source drain bias, there is a $0.25 \times G_0$ structure that develops at negative D.C. source drain bias. This asymmetry could be from self-consistent electrostatic effects close to channel pinch-off, or it could be caused by lateral spin-orbit coupling due to a small asymmetry in the confining potential. This asymmetric appearance of the $0.25 \times G_0$ could mean that a total spin polarisation is energetically unfavourable and a spin density wave or Skyrmion forms. Alternatively, a ferromagnetic ground state in an applied magnetic field with an interaction induced, spin-polarisation can be observed [28]. In GaAs devices under similar conditions a $0.25 \times G_0$ plateau usually forms rather than at $0.5 \times G_0$ and this has been explained as due to the source drain bias lifting the momentum degeneracy resulting in a unidirectional ferromagnetic order [29]. In this case a plateau appears at $0.5 \times G_0$ and stays with increasing D.C. source drain bias. There are anomalous plateaus in the conductance that show up at $0.8 \times G_0$ and $1.7 \times G_0$ in the conductance plot, see figure 2 (b). These behave in a similar way to the $0.7 \times G_0$ structure and are thought to be related to spin as a partially spin-polarized phase [30].

C. Applied magnetic fields

The magnetic field is applied in-plane and perpendicular to the effective Rashba field, i.e. along the 1-dimensional channel. This probes the low g-factor orientation and the effects of spin-orbit coupling should be clearer. 1-dimensional transport measurements [31] with an in-plane magnetic field show that in contrast to GaAs, only small magnetic fields are required to lift the spin degeneracy in InGaAs devices. Figure 3(a) shows a plot of the transconductance (dG/dV_{sg}) as the D.C. source drain bias is stepped from -8 mV to +8 mV in zero magnetic field. In figure 3(a) δV_g corresponds the difference in patterned gate voltage as the $N = 2$ and $N = 1$ subbands cross with finite V_{sd} . Figure 3(b) shows the

Zeeman splitting in the transconductance (dG/dV_{sg}) from 0 T to 8 T with $V_{sd} = 0$ V. In figure 3(b) δV_g corresponds the difference in patterned gate voltage as the $N = 2$ and $N = 1$ subbands cross in a parallel magnetic field. In $_{0.75}$ Ga $_{0.25}$ As devices require ~ 1.5 T of parallel magnetic field (B_{\parallel}) to lift the spin degeneracy compared with ~ 6 T for GaAs [31]. We obtain the g-factor using the technique developed in [26] which combines the measurement of the splitting due to the applied source drain bias with measurements where Zeeman splitting is due to the parallel magnetic field. The subband energy is measured by observing the splitting in gate voltage (δV_g) due to an applied D.C. source drain bias. The energy difference between spin-split energy levels is defined by the Zeeman energy (E_Z), see equation (1),

$$|g^*| = \frac{1}{\mu_B} \frac{dE_Z}{dB_{\parallel}} = \frac{1}{\mu_B} \frac{dE_Z}{dV_{sg}} \frac{dV_{sg}}{dB_{\parallel}} = \frac{e}{\mu_B} \frac{dV_{sd}}{dV_{sg}} \frac{dV_{sg}}{dB_{\parallel}} \quad (1)$$

e is the unit of charge. In figure 3(a), the subband spacing is shown to be between 3.6 meV and 2.5 meV. Larger values were reported in In $_{0.75}$ Ga $_{0.25}$ As/InP [32]. However, these devices were fabricated from etched wires that require a perpendicular magnetic field in order to reduce the disorder in the system and achieve quantised conductance [27, 33]. The term dV_{sg}/dB_{\parallel} can be estimated from figure 3(b). We obtain an effective g-factor of 6.5 for the lowest subband $N = 1$, and the data is obtained in the absence of Landau quantisation using finite perpendicular magnetic field. Table 1 is a summary for the lowest 3 subbands.

In a 2DEG with Rashba-type spin-orbit coupling, the band structure is split into two parabola, with a linear shift in k (the in-plane wave vector) with energies, $E^{\pm}(k)$ given by equation (2),

$$E^{\pm}(k) = \frac{\hbar^2 k^2}{2m^*} \pm \alpha k \quad (2)$$

where α is the Rashba parameter for this heterojunction system. In the In $_{0.75}$ Ga $_{0.25}$ As quantum well, the Rashba coefficient is 0.67×10^{11} eV.m with a spin-orbit splitting energy

of ~ 2.2 meV [8]. When this Rashba spin-orbit coupling is included in the calculation of the effective g-factor, this reduces the estimated value to 6 in the lowest subband ($N = 1$) for in-plane applied fields perpendicular to the Rashba field. The reduction in g-factor from the measured 2-dimensional value is due to the competition of Rashba and Zeeman magnetic fields. This reduction is one of the manifestations of the Rashba spin-orbit coupling effect that creates an effective magnetic field (~ 4 T), pinning the spin angular momentum in this in-plane direction [8].

D. Asymmetric patterned gate voltages

Asymmetric split-gate biasing was studied by stepping one patterned gate voltage and sweeping the second, see figure 4, where ΔV shows the difference in patterned gate voltage. We observe a weak spin-split $0.5 \times G_0$ plateau appearing, however this feature increases to $0.75 \times G_0$ as the channel is made more asymmetric. In addition there are plateaus which appear at $1.5 \times G_0$ and $3.5 \times G_0$ as the channel is made more asymmetric. The spin-split $0.5 \times G_0$ plateau has already been observed in an InAs quantum well with InGaAs barriers, when the confining potential was made asymmetric. This was ascribed to a lateral spin-orbit coupling effect [34]. However these measurements reported in reference [34] were made using etched channels with side gates. The etched wires have edges that are exposed to roughness and disorder and the spin-orbit length is smaller due to stronger confinement [35]. Spin-polarisation can be triggered by lateral spin-orbit coupling and lead to fully spin-polarised state in the presence of strong electron-electron interaction however this effect is not seen in these structures even though the measured Rashba spin-splitting energy is ~ 2.2 meV in this 2-dimensional system [8].

4. Conclusions

$\text{In}_{0.75}\text{Ga}_{0.25}\text{As}$ patterned gate devices investigated in this paper show the effects of spin-orbit interaction predominantly through a g-factor reduction rather than spin resolved conductance plateau at $0.5 \times G_0$ and higher conductance half plateaus. These experiments have determined the optimum device length scales to study quantised conductance with minimal effects from disorder and impurities that have plagued early studies of devices based on the InGaAs material system. These experiments have demonstrated that

1
2
3 $\text{In}_{0.75}\text{Ga}_{0.25}\text{As}$ patterned gate devices are suitable for future spintronic devices that require
4 only minimal applied magnetic fields. There is a reduction in backscattering due to spin-
5 orbit coupling at the 1-dimensional channel that leads to enhanced ballistic quantisation
6 up to a conductance of $6 \times (2e^2/h)$ even with appreciable disorder present.
7
8
9

10 11 12 13 **Acknowledgements**

14
15
16 The authors acknowledge financial support from the United Kingdom EPSRC (grant
17 EP/K004077/1). Y. Gul thanks Toshiba Research Europe Limited for the provision of an
18 EPSRC CASE award studentship.
19
20
21
22
23
24
25
26
27
28
29
30
31
32
33
34
35
36
37
38
39
40
41
42
43
44
45
46
47
48
49
50
51
52
53
54
55
56
57
58
59
60

References

- [1] Žutić Igor, Fabian Jaroslav, and Das Sarma S 2004 *Reviews of Modern Physics* **76** 323
- [2] Wang Chuan-Kui and Berggren K-F 1996 *Phys. Rev. B* **54** R14257
- [3] *Semiconductor Spintronics and Quantum Computation*, edited by Awschalom D D, Loss D, and Samarth N 2002 Springer Berlin Germany
- [4] Rashba E I 1960, *Sov. Phys. Solid State* **2** 1109
- [5] Bychkov Yu A and Rashba E I 1984 *JETP Lett.* **39** 78
- [6] Winkler R 2003 *Spin-Orbit Coupling Effects in Two-Dimensional Electron and Hole Systems* **191** Springer-Verlag, Berlin, Heidelberg
- [7] Flindt Christian, Sørensen Anders S, and Flensberg Karsten 2006 *Phys. Rev. Lett.* **97** 240501
- [8] Holmes S N, Simmonds P J, Beere H E, Sfigakis F, Farrer I, Ritchie D A, and Pepper M 2008 *J. Phys.: Condens. Matter* **20** 472207
- [9] Gozu Shin-ichirou, Hong Chulun and Yamada Syoji 1998 *Jpn. J. Appl. Phys.* **37** L1501
- [10] Wharam D, Thornton T J, Newbury R, Pepper M, Ahmed H, Frost J, Hasko D, Peacock D, Ritchie D A, and Jones G A C 1988 *J. Phys. C* **21** L209
- [11] Van Wees B J, Van Houten H, Beenakker C W J, Williamson J G, Kouwenhoven L P, van der Marel D, and Foxon C T 1988 *Phys. Rev. Lett.* **60** 848
- [12] Matveev K A 2004 *Phys. Rev. B* **70** 245319
- [13] Simmonds P J, Sfigakis F, Beere H E, Ritchie D A, Pepper M, Anderson D, and Jones G A C 2008 *Appl. Phys. Lett.* **92** 152108

- 1
2
3 [14] Simmonds P J, Holmes S N, Beere H E, Farrer I, Sfigakis F, Ritchie D A, Pepper M
4 2009 J. Vac. Sci. Technol. B **27** 2066
5
6
7 [15] Chen Chong, Farrer Ian, Holmes Stuart N, Sfigakis Francois, Fletcher Marc P, Beere
8 Harvey E, Ritchie David A 2015 J. Cryst. Growth **425** 70
9
10
11 [16] Kajiyama K, Mizushima Y, and Sakata S 1973 Appl. Phys. Lett. **23** 458
12
13
14 [17] Lehmann H, Benter T, von Ahnen I, Jacob J, Matsuyama T, Merkt U, Kunze U,
15 Wieck A D, Reuter D, Heyn C and Hansen W 2014 Semicond. Sci. Technol. **29** 075010
16
17
18 [18] Smith L W, Al-Taie H, Sfigakis F, See P, Lesage A A J, Xu B, Griffiths J P, Beere
19 H E, Jones G A C, Ritchie D A, Kelly M J, and Smith C G 2014 Phys. Rev. B **90** 045426
20
21
22 [19] Sasaki A, Nonaka S, Kunihashi Y, Kohda M, Bauernfeind T, Dollinger T, Richter K,
23 and Nitta J 2014 Nat. Nanotechnol. **9** 703
24
25
26 [20] Thomas K J, Nicholls J T, Simmons M Y, Pepper M, Mace D R, and Ritchie D A
27 1996 Phys. Rev. Lett. **77** 135
28
29
30 [21] Reilly D J 2005 Phys. Rev. B **72** 033309
31
32
33 [22] Aryanpour K and Han J E 2009 Phys. Rev. Lett. **102** 056805
34
35
36 [23] Sloggett C, Milstein A L, and Sushkov O P 2008 The European Physical Journal B
37 **61** 427
38
39
40 [24] Lunde A M, De Martino A, Schulz A, Egger R and Flensberg K 2009 New J. Phys.
41 **11** 023031
42
43
44 [25] Glazman L I and Khaetskii A V 1989 Europhys. Lett. **9** 263
45
46
47 [26] Patel N K, Nicholls J T, Martin-Moreno L, Pepper M, Frost J E F, Ritchie D A, and
48 Jones G A C 1991 Phys. Rev. B **44** 13549
49
50
51 [27] van Weperen Ilse, Plissard Sébastien R, Bakkers Erik P A M, Frolov Sergey M, and
52 Kouwenhoven Leo. P 2013 Nano Lett. **13** 387
53
54
55
56
57
58
59
60

1
2
3 [28] Renard V T, Piot B A, Waintal X, Fleury G, Cooper D, Niida Y, Tregurtha D,
4 Fujiwara A, Hirayama Y, and Takashina K 2015 Nat. Commun. **6** 7230
5

6
7
8 [29] Chen T-M, Graham A C, Pepper M, Farrer I, and Ritchie D A 2008 Appl. Phys. Lett.
9 **93** 032102
10

11
12 [30] Kristensen A, Bruus H, Hansen A E, Jensen J B, Lindelof P E, Marckmann C J,
13 Nygård J, Sørensen C B, Beuscher F, Forchel A, and Michel M 2000 Phys. Rev. B **62**
14 10950
15

16
17
18 [31] Pepper Michael and Bird Jonathan 2008 J. Phys.: Condens. Matter **20** 160301
19

20
21 [32] Martin T P, Szorkovszky A, Micolich A P, Hamilton A R, Marlow C A, Linke H,
22 Taylor R P, and Samuelson L 2008 Appl. Phys. Lett. **93** 012105
23

24
25 [33] Kohda M, Nakamura S, Nishihara Y, Kobayashi K, Ono T, Ohe J-i, Tokura Y,
26 Mineno T, and Nitta J 2012 Nat. Commun. **3** 1082
27

28
29
30 [34] Debray P, Rahman S M S, Wan J, Newrock R S, Cahay M, Ngo A T, Ulloa S E,
31 Herbert S T, Muhammad M, and Johnson M 2009 Nat. Nanotechnol. **4** 759
32

33
34 [35] Shabani J, Kim Younghyun, McFadden A P, Lutchyn R M, Nayak C, and
35 Palmstrøm C J 2014 arXiv:1408.1122v1
36
37
38
39
40
41
42
43
44
45
46
47
48
49
50
51
52
53
54
55
56
57
58
59
60

Figure captions

Figure 1 The differential conductance (G) in units of $2e^2/h$ as a function of patterned (split) gate voltage (V_{sg}) from 4.2 K to 50 mK in intervals of 0.05 K for the device with channel length 200 nm and patterned gate separation 400 nm. The conductance has been corrected for a series resistance and offset horizontally by 25 mV per set temperature. The dashed blue line indicates the $0.7 \times (2e^2/h)$ conductance feature.

Figure 2(a) D.C. bias spectroscopy of the device from 0 mV to 8 mV. The $0.5 \times (2e^2/h)$ conductance plateau is observed and remains from 3 mV with further plateaus developing at 1.5 , 2.5 and $3.5 \times (2e^2/h)$. **(b)** D.C. bias spectroscopy of the device from 0 mV to -8 mV. The $0.5 \times (2e^2/h)$ is again observed at ~ 3 mV, but tends to shift below $0.5 \times (2e^2/h)$ to $0.25 \times (2e^2/h)$ as the D.C. bias is increased.

Figure 3(a) The Transconductance (dG/dV_{sg}) as a function of gate voltage (V_{sg}) plotted against D.C. source drain bias (V_{sd}) with parallel magnetic field ($B_{||}$) set to 0. Regions of bright orange and red correspond to large amplitude dG/dV_{sg} , indicating the locations of subband transitions. **(b)** Transconductance (dG/dV_{sg}) as a function of gate voltage (V_{sg}) and parallel magnetic field ($B_{||}$). Regions of orange and red indicate large amplitude of dG/dV_{sg} corresponding to locations of subband transitions.

Figure 4 The device conductance as a function of asymmetric voltage to the patterned gates. One gate is held constant and the other gate is shifted incrementally up to $\Delta V = -2.8$ V at 50 mK in voltage steps of 20 mV.

Figures

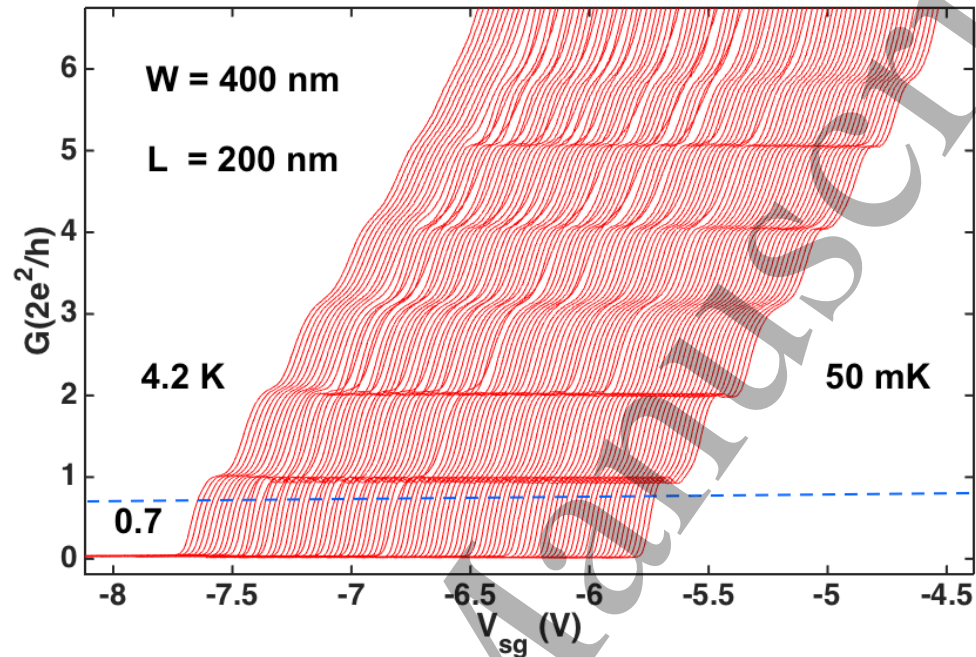


Figure 1.

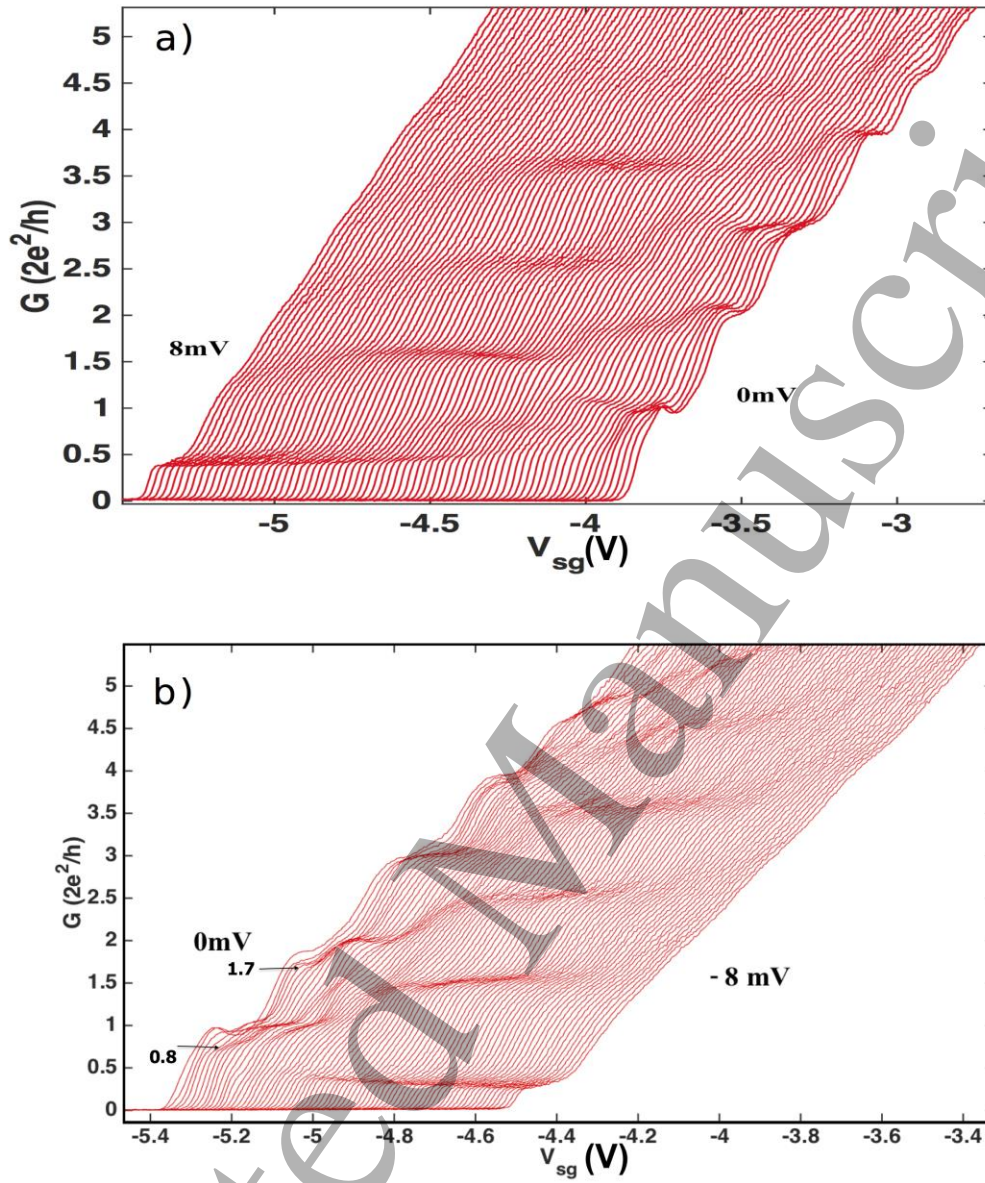


Figure 2.

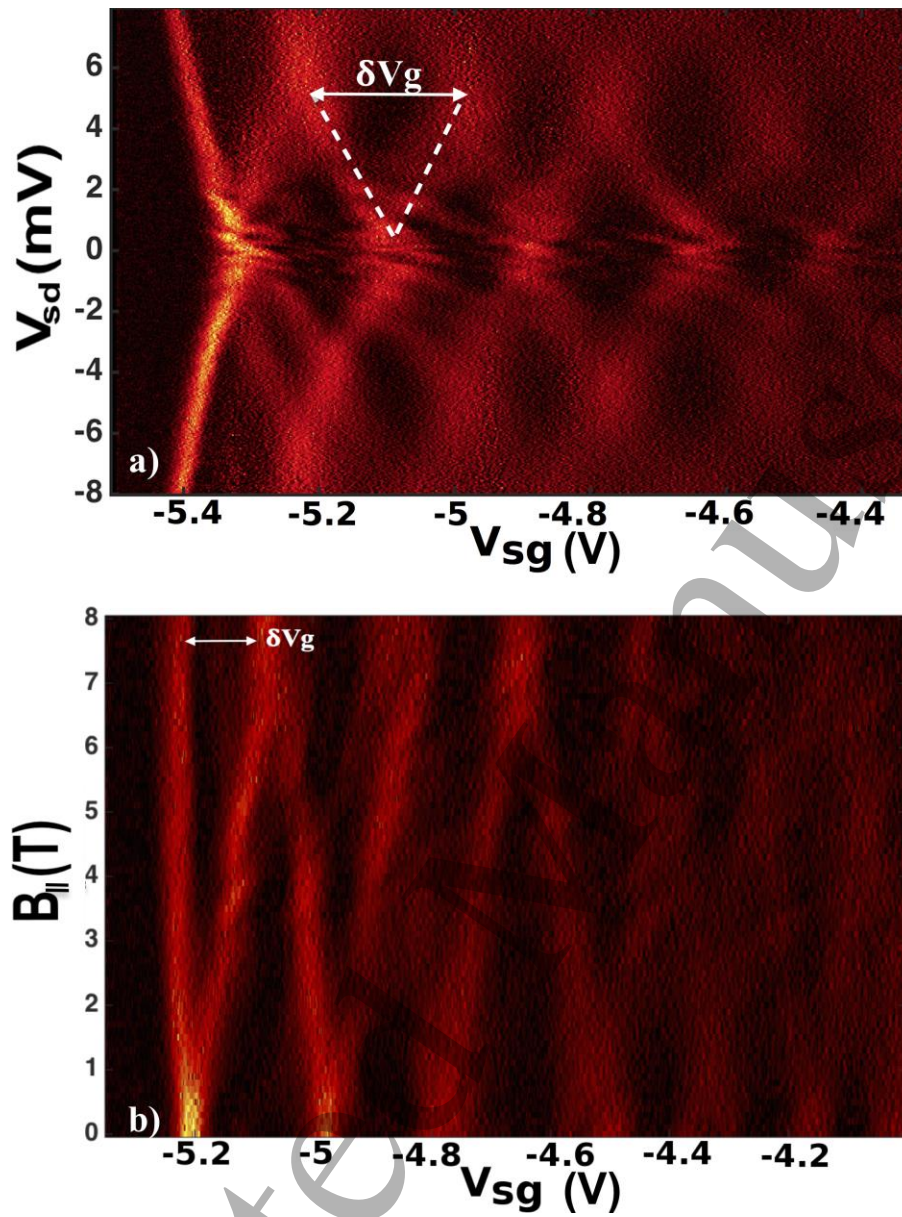


Figure 3.

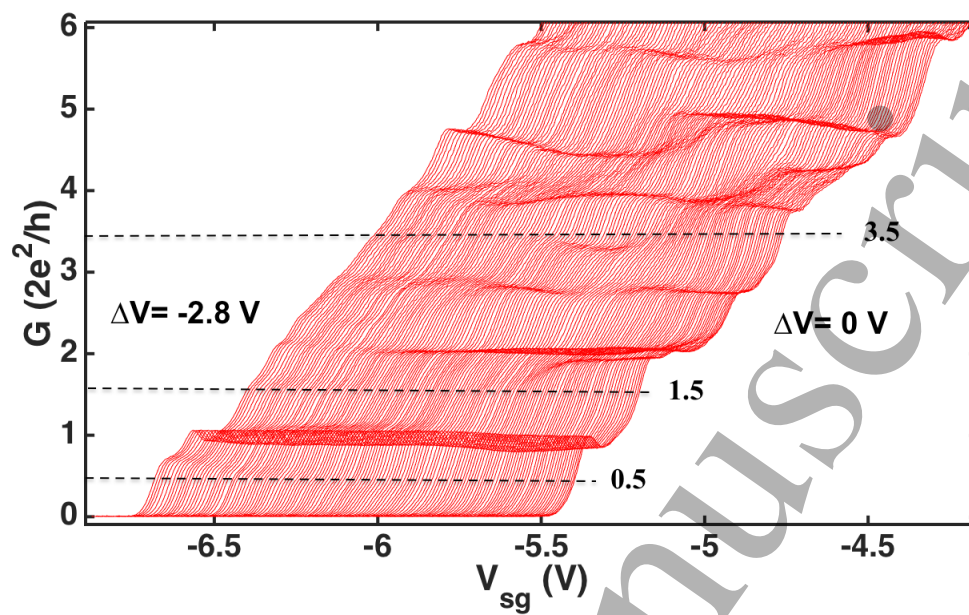


Figure 4.

Tables

subband	N=1	N=2	N=3
$\delta E_{n,n+1}$ (meV)	3.8	2.9	2.5
$\delta V_g/\delta B_{ }$ (V/T)	0.016	0.021	0.022
$\delta eV_{sd}/\delta V_g$ (meV/V)	23	17.1	12.8
$ g^* $	6.5	6.2	4.9

Table 1. Summary of the g-factors obtained for the first three sub-bands